Open Access Articles

PRC2 Is Required to Maintain Expression of the Maternal Gtl2-Rian-Mirg Locus by Preventing De Novo DNA Methylation in Mouse Embryonic Stem Cells

The Faculty of Oregon State University has made this article openly available.
Please share how this access benefits you. Your story matters.

Citation	Das, P. P., Hendrix, D. A., Apostolou, E., Buchner, A. H., Canver, M. C., Beyaz, S., ... & Orkin, S. H. (2015). PRC2 Is Required to Maintain Expression of the Maternal Gtl2-Rian-Mirg Locus by Preventing De Novo DNA Methylation in Mouse Embryonic Stem Cells. Cell Reports, 12(9), 1456-1470. doi:10.1016/j.celrep.2015.07.053
DOI	10.1016/j.celrep.2015.07.053
Publisher	Elsevier
Version	Version of Record
Terms of Use	http://cdss.library.oregonstate.edu/sa-termsofuse

Article

Cell Reports

PRC2 Is Required to Maintain Expression of the Maternal *Gtl2-Rian-Mirg* Locus by Preventing De Novo DNA Methylation in Mouse Embryonic Stem Cells

Graphical Abstract

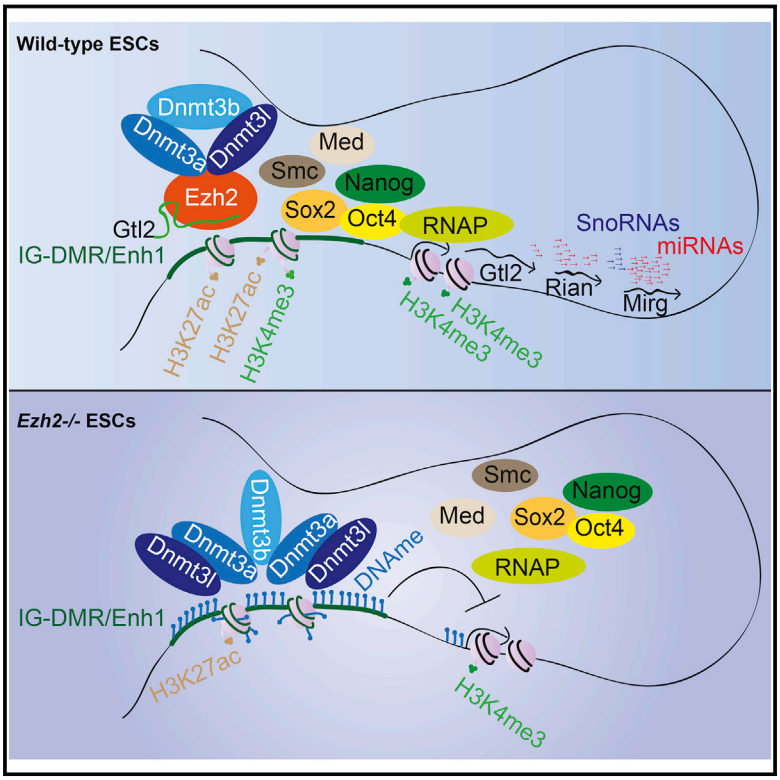

Highlights

- PRC2 is required to maintain expression of the maternal *Gtl2-Rian-Mirg* locus
- PRC2 transcriptionally regulates the *Gtl2-Rian-Mirg* locus through DNAme at IG-DMR
- IG-DMR serves as an enhancer of the maternal *Gtl2-Rian-Mirg* locus
- PRC2 prevents de novo DNAme at IG-DMR for maternal *Gtl2-Rian-Mirg* locus expression

Authors

Partha Pratim Das, David A. Hendrix, Effie Apostolou, ..., Konrad Hochedlinger, Jonghwan Kim, Stuart H. Orkin

Correspondence

stuart_orkin@dfci.harvard.edu

In Brief

Polycomb Repressive Complex 2 (PRC2) function and DNA methylation (DNAme) are both typically correlated with gene repression. Das et al. find that PRC2 prevents recruitment of Dnmt3s and DNAme at the IG-DMR element, thus allowing proper expression of the nearby maternal *Gtl2-Rian-Mirg* locus.

Accession Numbers

GSE58414

Das et al., 2015, Cell Reports *12*, 1456–1470
September 1, 2015 ©2015 The Authors
http://dx.doi.org/10.1016/j.celrep.2015.07.053

CrossMark

CellPress

OPEN ACCESS
CellPress

Cell Reports
Article

PRC2 Is Required to Maintain Expression of the Maternal *Gtl2-Rian-Mirg* Locus by Preventing De Novo DNA Methylation in Mouse Embryonic Stem Cells

Partha Pratim Das,[1,2,11] David A. Hendrix,[3,10,11] Effie Apostolou,[4,5,12] Alice H. Buchner,[1,6] Matthew C. Canver,[1] Semir Beyaz,[1] Damir Ljuboja,[1] Rachael Kuintzle,[10] Woojin Kim,[1] Rahul Karnik,[4,7] Zhen Shao,[1,13] Huafeng Xie,[1] Jian Xu,[1,14] Alejandro De Los Angeles,[1] Yingying Zhang,[4,7] Junho Choe,[8] Don Leong Jia Jun,[1,9] Xiaohua Shen,[1,15] Richard I. Gregory,[8] George Q. Daley,[1,2] Alexander Meissner,[4,7] Manolis Kellis,[3] Konrad Hochedlinger,[2,4,5] Jonghwan Kim,[1,16] and Stuart H. Orkin[1,2,*]

[1]Division of Hematology/Oncology, Boston Children's Hospital and Department of Pediatric Oncology, Dana-Farber Cancer Institute (DFCI), Harvard Stem Cell Institute, Harvard Medical School, Boston, MA 02115, USA
[2]Howard Hughes Medical Institute (HHMI), Boston, MA 02115, USA
[3]Computer Science and Artificial Intelligence Laboratory, Massachusetts Institute of Technology (MIT), Cambridge, MA 02139, USA
[4]Department of Stem Cell and Regenerative Biology, Harvard University and Harvard Medical School, 7 Divinity Avenue, Cambridge, MA 02138, USA
[5]Massachusetts General Hospital Cancer Center and Center for Regenerative Medicine, Boston, MA 02114, USA
[6]Molecular Biology Program, International Max Planck Research School, Georg-August-Universität Göttingen, Justus-von-Liebig-Weg 11, 37077 Göttingen, Germany
[7]Broad Institute, Cambridge, MA 02142, USA
[8]Stem Cell Program, Department of Biological Chemistry and Molecular Pharmacology and Department of Pediatrics, Boston Children's Hospital, Harvard Stem Cell Institute, Harvard Medical School, Boston, MA 02115, USA
[9]School of Chemical and Life Sciences, Singapore Polytechnic, 500 Dover Road, Singapore 139651, Singapore
[10]Department of Biochemistry and Biophysics, School of Electrical Engineering and Computer Science, Oregon State University, 2011 Ag and Life Science Building, Corvallis, OR 97331-7305, USA
[11]Co-first author
[12]Present address: Department of Medicine and Cancer Center, Weill Cornell Medical College, Belfer Research Building, 413 East 69th Street, New York, NY 10021, USA
[13]Present address: Key Laboratory of Computational Biology, CAS-MPG Partner Institute for Computational Biology, Shanghai Institutes for Biological Sciences, Chinese Academy of Sciences, Shanghai 200031, China
[14]Present address: Children's Medical Center Research Institute and Department of Pediatrics, The University of Texas Southwestern Medical Center, Dallas, TX 75235, USA
[15]Present address: Tsinghua-Peking Center for Life Sciences, School of Medicine, Tsinghua University, Beijing 100084, China
[16]Present address: Department of Molecular Biosciences, Institute for Cellular and Molecular Biology, Center for Systems and Synthetic Biology, The University of Texas, Austin, Austin, TX 78712, USA
*Correspondence: stuart_orkin@dfci.harvard.edu
http://dx.doi.org/10.1016/j.celrep.2015.07.053
This is an open access article under the CC BY license (http://creativecommons.org/licenses/by/4.0/).

SUMMARY

Polycomb Repressive Complex 2 (PRC2) function and DNA methylation (DNAme) are typically correlated with gene repression. Here, we show that PRC2 is required to maintain expression of maternal microRNAs (miRNAs) and long non-coding RNAs (lncRNAs) from the *Gtl2-Rian-Mirg* locus, which is essential for full pluripotency of iPSCs. In the absence of PRC2, the entire locus becomes transcriptionally repressed due to gain of DNAme at the intergenic differentially methylated regions (IG-DMRs). Furthermore, we demonstrate that the IG-DMR serves as an enhancer of the maternal *Gtl2-Rian-Mirg* locus. Further analysis reveals that PRC2 interacts physically with Dnmt3 methyltransferases and reduces recruitment to and subsequent DNAme at the IG-DMR, thereby allowing for proper expression of the maternal *Gtl2-Rian-Mirg* locus. Our observations are consistent with a mechanism through which PRC2 counteracts the action of Dnmt3 methyltransferases at an imprinted locus required for full pluripotency.

INTRODUCTION

Somatic cells are readily converted to an embryonic stem cell (ESC)-like state (induced pluripotent stem cells [iPSCs]) through enforced expression of a defined set of transcription factors (TFs), including Oct4, Sox2, Klf4, and c-Myc (OSKM) (Takahashi and Yamanaka, 2006). However, it remains unclear whether iPSCs are molecularly and functionally equivalent to blastocyst-derived ESCs. Overall mRNA and microRNA (miRNA) expression patterns are nearly indistinguishable between genetically

matched mouse ESCs (mESCs) and iPSCs, with the exception of a few maternally expressed long non-coding RNAs (lncRNAs Gtl2, Rian, and Mirg) and miRNAs originating from the imprinted *Dlk1-Dio3* gene cluster that is silenced in the majority of iPSC clones (Stadtfeld et al., 2010). The iPSC clones with a silenced *Dlk1-Dio3* gene cluster (called *Gtl2*^{OFF} clones) poorly contribute to chimeras and fail to yield viable iPSC-derived mice (all-iPSC mice). In contrast, iPSC clones with proper expression of the *Dlk1-Dio3* gene cluster (called *Gtl2*^{ON} clones) contribute to a high grade of chimeras and generate viable all-iPSC mice (Stadtfeld et al., 2010). Moreover, ascorbic acid (vitamin C) prevents the loss of imprinting at the *Dlk1-Dio3* gene cluster and facilitates generation of all-iPSC mice from differentiated B cells (Stadtfeld et al., 2012). Thus, expression of maternal lncRNAs and miRNAs from the *Dlk1-Dio3* imprinted gene cluster is essential for the establishment of full pluripotency. Here we find that Polycomb Repressive Complex 2 (PRC2) is required to maintain expression of the *Dlk1-Dio3* imprinted gene cluster, and that PRC2 counteracts de novo DNA methylation (DNAme) at this locus.

PRC2, which is comprised of the core components Ezh2/Ezh1, Eed, Suz12, histone chaperones Rbbp4/6, and associated other factors (e.g., Pcls and Jarid2), catalyzes H3K27me2/3, a chromatin mark correlated with transcriptional repression at silent and bivalent genes (Margueron and Reinberg, 2011). In ESCs, many PRC2 targets are bivalent and marked by both H3K4me3 and H3K27me3 at lineage-specific genes that are poised but activated upon differentiation (Boyer et al., 2006). As such, PRC2 is critical for both ESC maintenance and differentiation. Although bivalent domains initially were believed to be ESC specific, they have been identified in differentiated somatic cells at lower frequency (Bernstein et al., 2006; Mikkelsen et al., 2007). While most functions of PRC2 correlate with repression, a minority of studies implicate PRC2 in active transcription at a subset of its target genes in mESCs (Brookes et al., 2012; Ferrari et al., 2014).

The mechanism by which PRC2 is recruited to its target genes is incompletely understood. In *Drosophila*, Polycomb response elements (PREs) are responsible for PRC2 recruitment (Simon and Kingston, 2009). However, in mammals this is not the case. Instead, PRC2 is recruited at highly enriched CpG islands (Ku et al., 2008). Recent findings also posit that lncRNAs are important for PRC2 recruitment and its function. In mammals, X chromosome inactivation (XCI) initiates expression of the ~17-kb lncRNA Xist, which binds to PRC2 and catalyzes H3K27me3 in *cis* to control chromosome-wide silencing (Zhao et al., 2008). Also, repression of the *Hox-D* locus appears to be regulated in *trans* by Hotair that is generated from the *Hox-C* locus and binds to PRC2 (Rinn et al., 2007). In addition, a class of short RNAs (50–200 nt) plays an important role in association with PRC2 to regulate its target genes (Kanhere et al., 2010). Genome-wide analysis using RNA immunoprecipitation (RIP) sequencing demonstrates >9,000 lncRNAs (>200 nt in size) are associated with PRC2 (Zhao et al., 2010). The PRC2-interacting transcriptome consists of numerous transcripts, such as Xist, H19, Igf2, Air, Igf2r, Kcnq1, and Gtl2, that originate from genomic imprinted loci (Zhao et al., 2010). Genomic imprinting is an epigenetic phenomenon in which genes are expressed either from the paternally or maternally inherited allele (Edwards and Ferguson-Smith, 2007). The majority of imprinted genes are clustered in the genome and usually contain protein-coding genes as well as at least one non-coding RNA (ncRNA) (Edwards and Ferguson-Smith, 2007). Each cluster is under the control of a *cis*-regulatory element, termed the imprinting control region (ICR). ICRs generally acquire DNAme during oogenesis or spermatogenesis in germ cells and that leads to imprinting of one of the parental alleles (da Rocha et al., 2008). The detailed functions of PRC2 lncRNAs in mediating the regulation of genomic imprinting are largely unknown. For example, PRC2-Gtl2 lncRNA represses *Dlk1* expression in *cis* (Zhao et al., 2010); similarly, Kcnq1ot1 lncRNA interacts with PRC2 and silences genes in the *Kcnq1* domain in *cis* (Pandey et al., 2008).

Contrary to the conventional role of PRC2 in maintenance of repression, we demonstrate here that PRC2 is required to maintain expression of maternal miRNAs and lncRNAs from the *Gtl2-Rian-Mirg* locus within the *Dlk1-Dio3* imprinted gene cluster in mESCs. In the absence of Ezh2/PRC2, the entire *Gtl2-Rian-Mirg* locus becomes transcriptionally silent due to gain of de novo DNAme at the IG-DMR, a critical *cis*-regulatory element that controls expression of the maternal *Gtl2-Rian-Mirg* locus. In the presence of PRC2, the maternal IG-DMR is lowly methylated and acts as an enhancer of the maternal *Gtl2-Rian-Mirg* locus. Further analysis shows that PRC2 prevents Dnmt3 methyltransferase recruitment and subsequent de novo DNAme at the IG-DMR, thereby allowing proper expression of the maternal *Gtl2-Rian-Mirg* locus. These findings reveal an unanticipated function of PRC2 as well as the complex interplay between PRC2 function and DNAme. Our observations suggest a mechanism through which PRC2 antagonizes de novo DNAme at an imprinted locus.

RESULTS

PRC2 Is Required to Maintain Expression of Maternal miRNAs and lncRNAs at the *Gtl2-Rian-Mirg* Locus

To further investigate the role of PRC2 in gene regulation in mESCs, we conducted both RNA and size-selected small RNA expression profiling using high-throughput sequencing of *Ezh2*−/− and wild-type mESCs. We observed a striking reduction in expression of a cluster of miRNAs in *Ezh2*−/− mESCs at the *Gtl2-Rian-Mirg* locus within the *Dlk1-Dio3* imprinted gene cluster on chromosome 12qf1 (Figures 1A and 1B). The *Gtl2-Rian-Mirg* locus harbors lncRNA genes (*Gtl2*, *Rian*, and *Mirg*), miRNAs, and small nucleolar RNAs (snoRNAs) that are expressed from the maternally inherited chromosome, whereas protein-coding genes *Dlk1* and *Dio3* are expressed from the paternally inherited chromosome (Figure 1B; da Rocha et al., 2008). Furthermore, global qRT-PCR analysis of total miRNA expression per chromosome revealed a significant reduction in miRNA expression from chromosome 12 in *Ezh2*−/− mESCs (Figure S1B), as the majority of the miRNAs reside at the maternal *Gtl2-Rian-Mirg* locus of chromosome 12. We also observed a reduced expression of maternal miRNAs derived from the *Gtl2-Rian-Mirg* locus, as well as from chromosome 12, in *Eed*−/− and *Jarid2*−/− mESCs (Figures S1A and S1B). Northern blot and qRT-PCR confirmed reduced expression of selected maternal miRNAs (miR-127, miR-134, miR-323-3p,

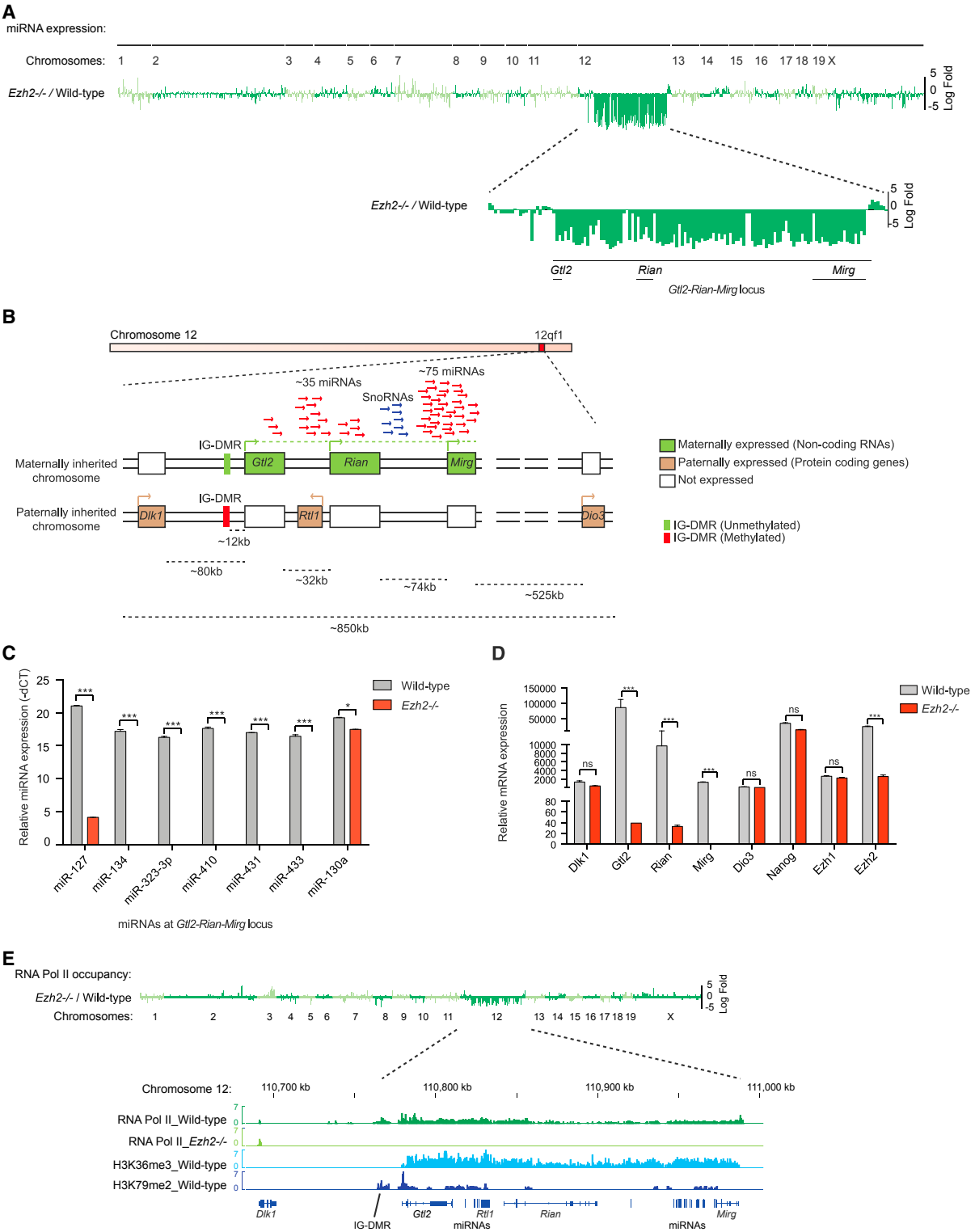

Figure 1. PRC2 Is Required to Maintain Expression of Maternal miRNAs and lncRNAs at the *Gtl2-Rian-Mirg* Locus

(A) Small RNA-seq demonstrates log-fold changes of miRNA expression in *Ezh2*−/− mESCs compared to wild-type. Significantly reduced expression of a cluster of miRNAs is observed at the *Gtl2-Rian-Mirg* locus of chromosome 12 in *Ezh2*−/− mESCs compared to wild-type.

(B) Schematic representation of the *Dlk1-Dio3* imprinted gene cluster. The lncRNA genes (*Gtl2*, *Rian*, and *Mirg*), miRNAs, and snoRNAs are expressed from maternally inherited chromosome, whereas protein-coding genes, *Dlk1*, *Dio3*, and *Rtl1*, are expressed from paternally inherited chromosome. Empty boxes

(legend continued on next page)

miR-410, miR-431, and miR-433) in *Ezh2*−/−, as well as in *Eed*−/− and *Jarid2*−/−, mESCs as compared to wild-type (Figures 1C and S1C–S1E). Another independent *Ezh2*−/− clone showed similar levels of reduction of all these maternal miRNAs (Figure S1H). To exclude possible effects on miRNA biogenesis in the absence of PRC2, we examined expression of Dicer, Drosha, and Ago2. Expression of these critical factors for miRNA biogenesis was unchanged in the absence of PRC2 (Figure S1F).

Next we examined expression of lncRNAs Gtl2 (also known as Meg3), Rian, and Mirg, as well as protein-coding genes *Dlk1* and *Dio3*. RNA sequencing (RNA-seq) and qRT-PCR revealed a marked reduction in expression of the maternal Gtl2, Rian, and Mirg lncRNAs in two independent *Ezh2*−/− mESC clones, similar to the observed deficit in miRNA expression in these cells. However, expression of the paternal Dlk1 and Dio3 alleles was unaffected (Figures 1D, S1G, and S1I). Similarly, expression of Gtl2, Rian, and Mirg lncRNAs also was reduced in *Eed*−/− and *Jarid2*−/− mESCs (Figures S1G and S1J). The deficit in expression of miRNAs and lncRNAs was greater in the absence of Ezh2 as compared to Eed or Jarid2 loss. Marked reduction in expression of maternal miRNAs and lncRNAs from the *Gtl2-Rian-Mirg* locus in the absence of several PRC2 components implies that transcription of the entire locus was affected in the absence of intact PRC2.

To establish this, we performed chromatin immunoprecipitation sequencing (ChIP-seq) analysis of RNA Polycomb II (Pol II), which revealed a significant reduction of RNA Pol II occupancy at the entire *Gtl2-Rian-Mirg* locus (~220 kb) in *Ezh2*−/− mESCs compared to wild-type (Figure 1E). Thus, the entire maternal *Gtl2-Rian-Mirg* locus is repressed in the absence of Ezh2/PRC2. Interestingly, RNA Pol II co-occupied with H3K36me3 and H3K79me2 elongation marks at the *Gtl2-Rian-Mirg* locus (Zhou et al., 2011; Figure 1E). This continuous stretch of co-occupancy of RNA Pol II, H3K36me3, and H3K79me2 and sense-strand specificity of maternal miRNAs and lncRNAs indicate that the maternal *Gtl2-Rian-Mirg* locus may act as a single transcriptional unit, and most likely maternal miRNAs and lncRNAs are processed from this single transcript. Moreover, a global view of mRNA expression analysis of all imprinted genes showed differential expression of selected imprinted genes in the absence of PRC2 components (Figure S1K). The most pronounced reduction in expression was observed at the *Gtl2-Rian-Mirg* locus in the absence of Ezh2, Eed, and Jarid2 of the PRC2 components; H19 expression was significantly reduced, but only in the absence of Ezh2 or Jarid2 (Figures S1K and S1L).

Methylation of the *Gtl2-Rian-Mirg* Locus in the Absence of PRC2

To explore mechanisms by which PRC2 loss might lead to repression of the *Gtl2-Rian-Mirg* locus, we first attempted to rescue Ezh2 expression in *Ezh2*−/− mESCs. Individual Ezh2 rescue clones expressing different levels of exogenous Ezh2 were examined (Figures S2A and S2C). Ezh2 rescue clones with low-level Ezh2 expression failed to rescue expression of maternal lncRNAs and miRNAs (Figures 2A and 2B). Even Ezh2 rescue clones (clones A5 and B6) that expressed at a near-endogenous level of Ezh2 and restored global H3K27me3 failed to rescue maternal Gtl2, Rian, and Mirg lncRNAs, as well as miRNA expression from the *Gtl2-Rian-Mirg* locus (Figures 2A, 2B, and S2B–S2E).

To study the basis for highly inefficient rescue of maternal lncRNAs and miRNAs upon re-expression of Ezh2, we assessed DNAme level at the IG-DMR, an important regulatory element located ~12 kb upstream of the *Gtl2* promoter involved in regional imprinting at the *Gtl2-Rian-Mirg* locus. The IG-DMR of the paternally inherited chromosome was heavily methylated. In contrast, the IG-DMR on the maternally inherited chromosome remained unmethylated (Figure 1B; Lin et al., 2003; da Rocha et al., 2008). As expected, the IG-DMR was 45% DNA methylated in wild-type mESCs. However, the methylation level increased to 92% in *Ezh2*−/− mESCs. Ezh2 rescue clones A5 and B6, which expressed near-endogenous levels of Ezh2, retained 92% and 88% DNAme at the IG-DMR, respectively (Figure 2C). Furthermore, treatment with high concentrations of the Dnmt inhibitor 5-azacitidine (5-aza) failed to restore Gtl2 expression in *Ezh2*−/− mESCs and Ezh2 rescue clones (Figure S2F). Similarly, high concentrations of ascorbic acid (vitamin C) failed to restore Gtl2 expression in *Ezh2*−/− (Figure S2G). Thus, DNAme at the IG-DMR is both dense and stable in the absence of Ezh2. Moreover, we observed a small increase in H3K9me3 occupancy at the IG-DMR locus in *Ezh2*−/− mESCs as compared to wild-type (Figure S2H), suggesting that co-operation between DNAme and H3K9me3 may lead to stable and long-term silencing of the maternal *Gtl2-Rian-Mirg* locus (Epsztejn-Litman et al., 2008; Dong et al., 2008; Smith and Meissner, 2013) in the absence of Ezh2. These data imply that DNAme is stable at the IG-DMR in the absence of Ezh2 and causes repression of lncRNAs and miRNAs. Once DNAme is established, re-expression of Ezh2 is unable to erase DNAme from the IG-DMR. Taken together, these results indicate that PRC2 is required to maintain expression of the maternal *Gtl2-Rian-Mirg* locus, most likely through preventing DNAme at the IG-DMR.

represent genes that are repressed. Imprinting is regulated by IG-DMR, which is methylated in paternally inherited chromosome, but unmethylated in maternally inherited chromosome. Therefore, by default, all lncRNAs, miRNAs, and snoRNAs from paternally inherited chromosome are repressed due to hypermethylation at IG-DMR, and only maternal ones are expressed.

(C) The qRT-PCR confirms dramatically reduced expression of maternal miRNAs from the *Gtl2-Rian-Mirg* locus in *Ezh2*−/− mESCs; miR-130a is shown as a control. miRNA expression is represented as mean ± SEM (n = 3); p values were calculated using a two-way ANOVA; ***p < 0.0001, *p < 0.01.

(D) The qRT-PCR shows a dramatic reduction of maternal Gtl2, Rian, and Mirg lncRNA expression in *Ezh2*−/− mESCs as compared to wild-type. Dlk1 and Dio3 mRNA expression is unaltered in *Ezh2*−/− mESCs. Transcript levels were normalized to Gapdh. Data are represented as mean ± SEM (n = 3); p values were calculated using a two-way ANOVA; ***p < 0.0001; ns, non-significant.

(E) ChIP-seq analysis of RNA Pol II demonstrates log-fold changes of RNA Pol II occupancy in *Ezh2*−/− mESCs compared to wild-type. RNA Pol II occupancy is significantly reduced at the entire *Gtl2-Rian-Mirg* locus (~220 kb) in *Ezh2*−/− mESCs compared to wild-type. RNA Pol II co-occupancy with H3K36me3 and H3K79me2 (elongation marks) suggests that the maternal *Gtl2-Rian-Mirg* locus acts as a single transcriptional unit.

See also Figure S1.

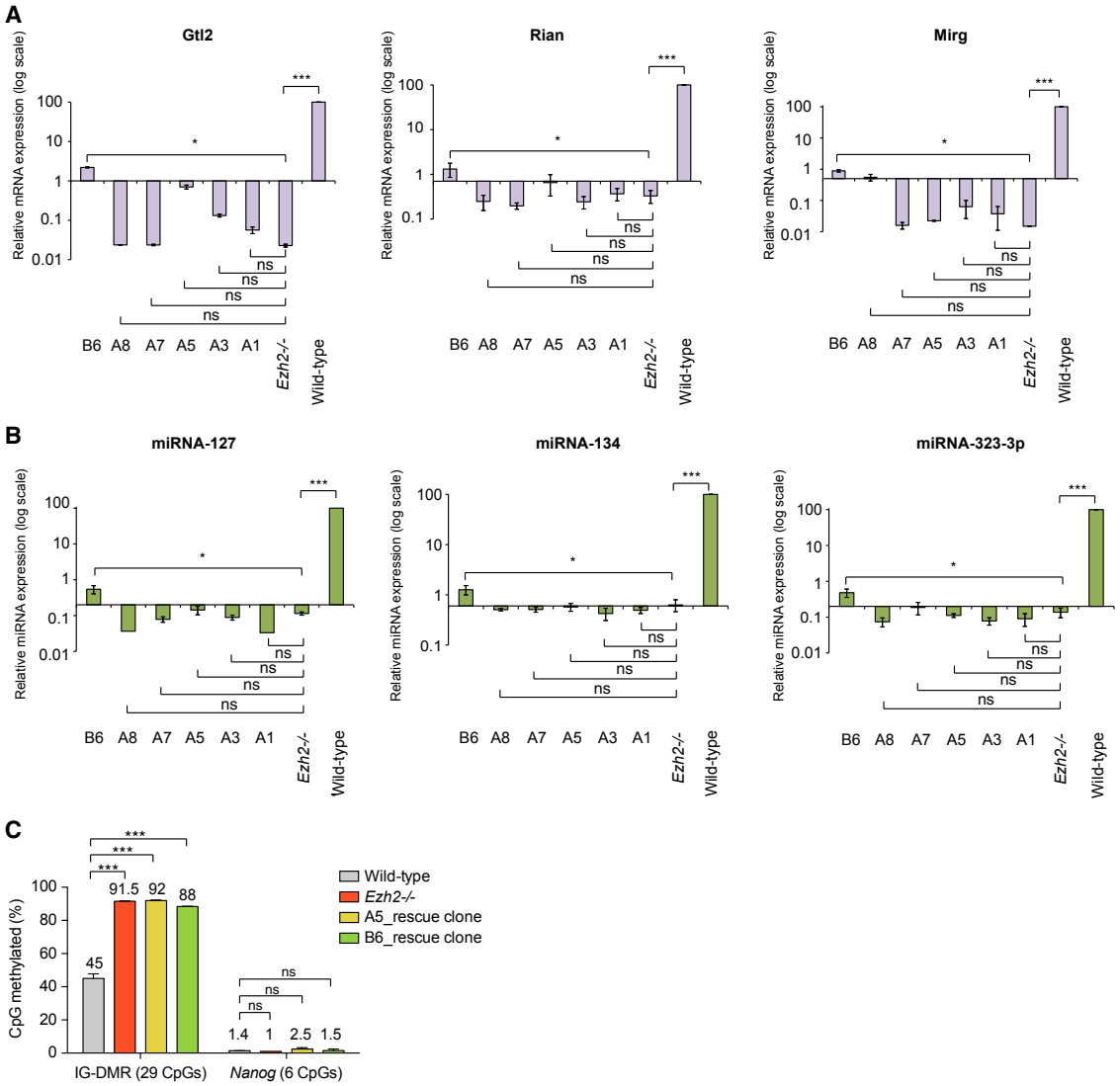

Figure 2. Methylation of the *Gtl2-Rian-Mirg* Locus in the Absence of PRC2

(A and B) Several independent Ezh2 rescue clones express different levels of exogenous Ezh2 (Figures S2A and S2C). Rescue clones with lower levels of Ezh2 expression fail to rescue the expression of maternal lncRNAs and miRNAs. Ezh2 rescue clones A5 and B6, which express at a near-endogenous level of Ezh2 (Figures S2A and S2C), also fail to restore the expression of maternal Gtl2, Rian, and Mirg lncRNAs (A) as well as miRNAs from the *Gtl2-Rian-Mirg* locus (B). mRNA transcript levels were normalized to Gapdh. Both mRNA and miRNA expressions are shown as mean ± SEM (n = 3); p values were calculated using a one-way ANOVA; ***p < 0.0001, *p < 0.01; ns, non-significant.

(C) Analysis of 29 CpGs at the IG-DMR shows gain of DNAme (%) in *Ezh2−/−* mESCs compared to wild-type. Ezh2 rescue clones A5 and B6, which express similar levels of endogenous Ezh2, retain hypermethylation at IG-DMR, indicating stable establishment of DNAme at the IG-DMR in the absence of Ezh2. DNAme at *Nanog* proximal promoter was used as a control. Data are represented as mean ± SEM (n = 3); p values were calculated using a two-way ANOVA; ***p < 0.0001; ns, non-significant.

See also Figure S2.

IG-DMR/Enhancer1 Serves as an Enhancer for the *Gtl2-Rian-Mirg* Locus

DNAme at the IG-DMR has been established as essential for proper imprinting control (Lin et al., 2003; da Rocha et al., 2008). However, the role of histone modifications at the IG-DMR in imprinting is less well understood. We examined the binding landscape of ESC-specific pluripotency factors, cohesion, mediators, histone marks, and PRC2 components at the entire *Dlk1-Dio3* gene cluster (Figures 3A and S3A). The IG-DMR was co-occupied by ESC-specific TFs (e.g., Oct4, Nanog, Sox2, Klf4, and Esrrb), mediator (Med1/12), cohesin (Smc1/3), Lsd1, H3K27ac, and H3K4me1 (Figures 3A–3C). Taken together, these characteristics are consistent with this region serving as an enhancer (Kagey et al., 2010; Whyte et al., 2012). We designated this region Enhancer1 (Enh1). A similar region (Enhancer2 [Enh2]), located farther downstream (~450 kb) of Enh1, showed

similar binding patterns (Figure 3D). Both Enh1 and Enh2 exhibited strong enhancer activity in reporter assays (Figure 3E). Interestingly, we observed that the H3K27ac mark was significantly reduced at Enh1 and Enh2 in *Ezh2*−/− mESCs. This finding correlates with reduced expression of maternal lncRNAs and miRNAs from the *Gtl2-Rian-Mirg* locus in the absence of Ezh2, suggesting that the H3K27ac active histone mark is an indicator of transcription activity of this imprinted locus (Figures 3C and 3D; Xie et al., 2012). Of note, we observed reduced marking with H3K27ac and H3K4me3, as well at the *Gtl2* promoter in the absence of Ezh2/PRC2. Strikingly, we found weak occupancy of Ezh2, Jarid2, and no binding of Suz12 of PRC2 components at IG-DMR/Enh1 and Enh2, and we failed to observe detectable H3K27me3 deposition (Figures 3C and 3D). We cannot exclude the possibility that the weak binding of Ezh2/PRC2 we saw derives from the paternal allele.

The similarities between Enh1 and Enh2 led us to consider how together they might regulate the maternal *Gtl2-Rian-Mirg* locus. However, unlike IG-DMR/Enh1, Enh2 is not hypermethylated in the absence of Ezh2 (Figure S3B). We investigated whether Enh1 and Enh2 loop into proximity with the *Gtl2* promoter to regulate the *Gtl2-Rian-Mirg* locus. Chromosomal conformation capture (3C) revealed that both Enh1 and Enh2 interact with the *Gtl2* promoter in the presence and absence of Ezh2 (Figure S3C), suggesting that Ezh2 does not interfere with looping between *Gtl2* promoter and Enh1/Enh2. To determine a requirement for IG-DMR/Enh1 and Enh2 in regulation of the *Gtl2-Rian-Mirg* locus, we deleted Enh1 (7 kb) and Enh2 (7 kb) using the clustered regularly interspaced short palindromic repeats (CRISPR)/Cas9 nuclease system (Cong et al., 2013). Biallelic deletion of Enh2 (Enh2−/−) failed to affect expression of the *Gtl2-Rian-Mirg* locus. In contrast, biallelic deletion of IG-DMR/Enh1 (IG-DMR/Enh1−/−) abrogated expression of maternal Gtl2, Rian, and Mirg (Figure 3F), demonstrating that IG-DMR/Enh1 is an essential regulatory element for the maternal *Gtl2-Rian-Mirg* locus (Lin et al., 2003). We identified strong co-occupancy of PRC2 and H3K27me3 at the *Dlk1* promoter (Figures 3A and 3B). Therefore, we hypothesized that PRC2 might distally regulate the *Gtl2-Rian-Mirg* locus. To test this possibility, we deleted the *Dlk1* promoter region (3 kb) using CRISPR/Cas9. Biallelic deletion of the *Dlk1* promoter showed no effect on the locus (Figure S3D), indicating that PRC2 does not distally regulate the *Gtl2-Rian-Mirg* locus. Collectively, these results demonstrate that the IG-DMR/Enh1 is an important *cis*-regulatory element that serves as an enhancer for the maternal *Gtl2-Rian-Mirg* locus.

PRC2 Physically Interacts with Dnmt3a/3l in a Gtl2 lncRNA-Independent Manner, and the Interaction between Gtl2 lncRNA-Ezh2 Inhibits Binding of Ezh2/PRC2 at the IG-DMR

Our results demonstrate that, in the absence of PRC2, the entire maternal *Gtl2-Rian-Mirg* locus is transcriptionally repressed in association with DNA hypermethylation at the IG-DMR (Figures 1 and 2). These data hint at a strong connection between DNAme and PRC2 in regulation of this locus. To explore this relationship further, we examined expression of DNA methyltransferases (Dnmts) in *Ezh2*−/− and wild-type mESCs. We found that expression of the de novo Dnmts, particularly Dnmt3a and Dnmt3l, were upregulated in *Ezh2*−/− mESCs (Figures 4A and 4B). Expression of Dnmt1, which is responsible for DNAme maintenance, was not significantly altered in *Ezh2*−/− mESCs (Figures 4A and 4B). Additionally, we observed upregulation of Dnmt3a and Dnmt3l in *Eed*−/− and *Jarid2*−/− mESCs (Figure S4A). Ezh2 expression was unaffected in the absence of any Dnmts (Figure S4B). Co-immunoprecipitation revealed that Ezh2, as well as Jarid2, interacts with Dnmt3a/Dnmt3l proteins (Figures 4C, S4C, and S4E). Moreover, Dnmt3a and Dnmt3l were both eluted in the same fractions as PRC2 components (Ezh2, Jarid2, and Suz12) (Figure S4D), consistent with interaction between PRC2 and Dnmt3a/3l.

We asked whether interaction between Ezh2 and Dnmt3a/3l is dependent on Gtl2 lncRNA. To test this, we used biallelic IG-DMR−/− mESCs, in which expression of maternal Gtl2 lncRNA is abrogated (Figures 3F and 4D). Interaction between Ezh2 and Dnmt3a/Dnmt3l was observed in the absence of Gtl2 lncRNA (Figure 4D). Nonetheless, Gtl2 lncRNA bound to PRC2 components (Ezh2, Eed, and Suz12), but not detectably to Dnmt3a (Figures 4E and S4F). Thus, the interaction between PRC2 and Dnmt3a/3l is Gtl2 lncRNA independent. Of note, interactions between Gtl2 lncRNA and PRC2 components (Ezh2, Eed, and Suz12) (Figure S4F), as well as interactions between PRC2 components (Figure S4E), suggest that assembly or interactions of PRC2 complex components are not prevented in the presence of Gtl2 lncRNA.

PRC2 transcriptome analysis identified a genome-wide pool of >9,000 PRC2-interacting RNAs, including Gtl2 lncRNA, in mESCs (Zhao et al., 2010). The majority of these PRC2-interacting RNAs recruit PRC2 itself at their targets for gene repression (Margueron and Reinberg, 2011). However, recent studies demonstrated that Ezh2/PRC2 is located at a large fraction of active promoters, where it binds to the nascent RNAs that somehow reduce deposition of H3K27me3 (Davidovich et al., 2013; Kaneko et al., 2013). Interestingly, these active promoters reveal low-level occupancy by Ezh2 (Kaneko et al., 2013). Further studies showed that deletion of PRC2-interacting RNA/s rescued PRC2-mediated deposition of H3K27me3 (Kaneko et al., 2014), implying that PRC2 activity is inhibited by interaction with nascent transcripts. We hypothesized that similar binding of nascent Gtl2 lncRNA to Ezh2 (Figure 4E) inhibits the interaction of Ezh2/PRC2 at the IG-DMR and subsequent deposition of H3K27me3. To support this, we showed that *Gtl2* promoter deletion disrupts the formation of Gtl2 lncRNA and is associated with increased binding of Ezh2 at the IG-DMR locus (Figures 4F and 4G). We did not observe, however, a significant increase in H3K27me3 at the IG-DMR (Figure 4H).

PRC2 Antagonizes De Novo DNAme at the IG-DMR through a Distinct Mechanism

Next we determined the occupancy of Dnmt3a, Dnmt3b, Dnmt3l, and Dnmt1 at the IG-DMR locus in the absence of PRC2. Occupancy of Dnmt3a, Dnmt3b, and Dnmt3l was markedly increased at the IG-DMR locus in the absence of Ezh2 or Jarid2 (Figures 5A and 5B). We noted that recruitment of Dnmt3a/3b/3l was higher at the IG-DMR in the absence of Ezh2 as compared to the absence of Jarid2, which may indicate

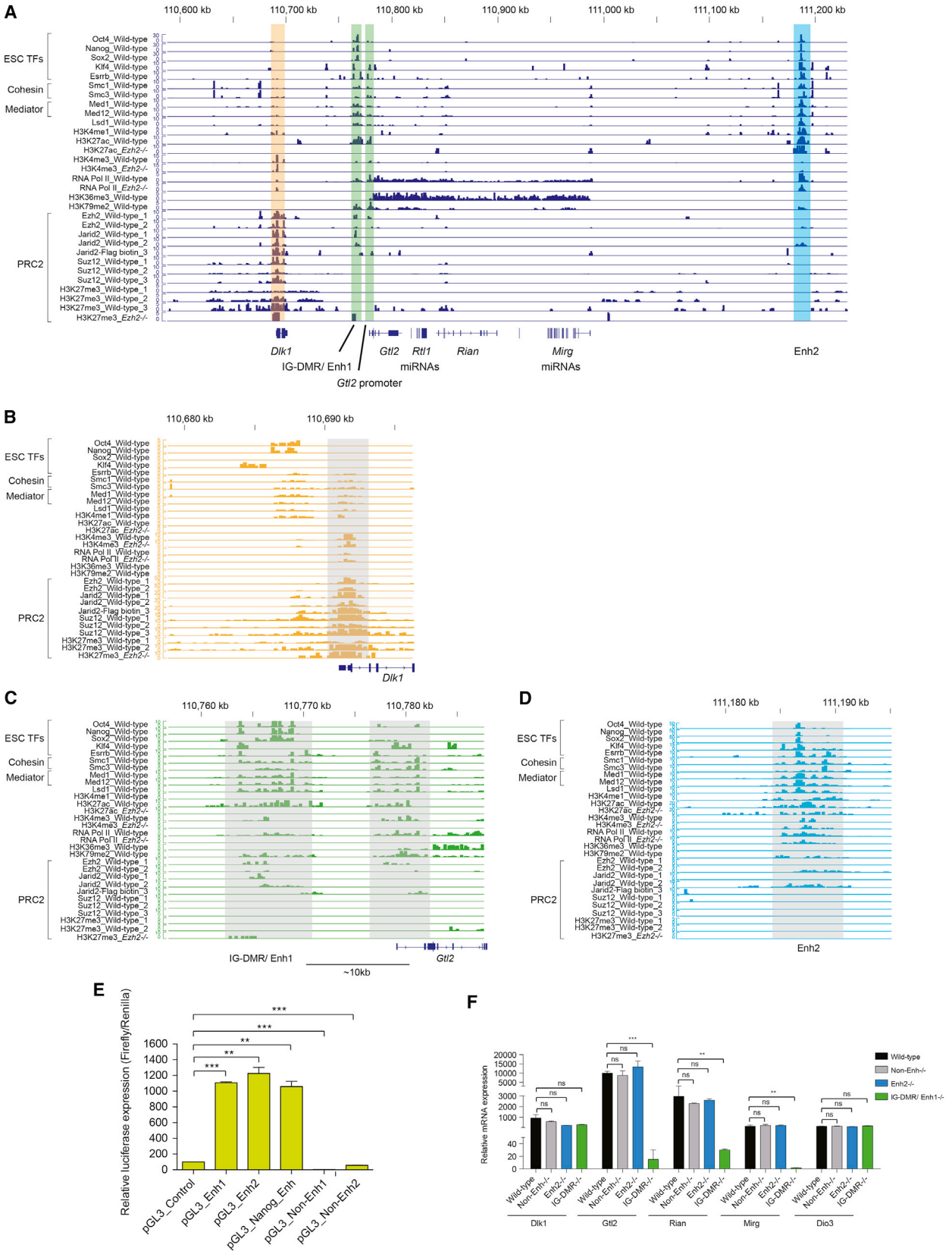

(legend on next page)

that components of PRC2 have different capacities to modulate de novo Dnmt3s occupancy/recruitment at the IG-DMR. We pursued this observation further by examining DNAme levels at the IG-DMR in *Ezh2*−/−, *Eed*−/−, and *Jarid2*−/− mESCs. Indeed, different extents of DNA hypermethylation were observed at the IG-DMR in the absence of the distinct PRC2 components (Figure 5C). Importantly, DNA hypermethylation levels at the IG-DMR correlated with reduced expression levels of maternal lncRNAs and miRNAs at the *Gtl2-Rian-Mirg* locus in the absence of Ezh2, Eed, and Jarid2 (Figures 1 and S1). In summary, these data suggest that PRC2 prevents recruitment of Dnmt3s for de novo DNAme at the IG-DMR to allow proper expression of the maternal *Gtl2-Rian-Mirg* locus.

To exclude the trivial possibility that increased binding of Dnmt3 methyltransferases and DNAme at the IG-DMR is due to increased levels of de novo Dnmt3 methyltransferases in the absence of Ezh2, we performed global DNAme analysis from *Ezh2*−/− and wild-type mESCs using reduced-representation bisulfite sequencing (RRBS). We observed a gain of DNAme globally in the absence of Ezh2 (Figure 5D). Particularly, DNAme was gained at Ezh2-binding sites, in the absence of Ezh2 (Figure S5G). These data indicate the Ezh2 antagonizes Dnmt3 methyltransferase activity and DNAme in mESCs.

To investigate whether this mechanism is restricted to the maternal *Gtl2-Rian-Mirg* imprinted locus, we examined histone marks, PRC2 occupancy, and DNAme at several differentially regulated imprinted loci, including *H19*, whose expression also significantly was reduced in the absence of PRC2 (Figure S1K). Occupancy of H3K27ac and H3K4me3 was significantly reduced at both the ICRs, IG-DMR (for *Gtl2-Rian-Mirg* locus) and ICR (for *H19*) in the absence of Ezh2, correlating with reduced expression of Gtl2, Rian, and H19. Interestingly, the ICR of *H19* was strongly occupied by Ezh2/PRC2 with corresponding H3K27me3 deposition and acquired DNAme in the absence of Ezh2/PRC2, whereas the IG-DMR was weakly occupied by Ezh2/PRC2 without H3K27me3 yet gained DNAme in the absence of Ezh2/PRC2 (Figures S5A–S5F). These findings are consistent with antagonism between PRC2 and DNAme at both loci, but they hint at differences in mechanistic detail.

PRC2 Protects IG-DMR from De Novo DNAme to Allow Proper Expression of the Maternal *Gtl2-Rian-Mirg* Locus

We demonstrated that Gtl2 lncRNA inhibits strong Ezh2/PRC2 occupancy and subsequent H3K27me3 deposition at the IG-DMR locus (Figures 3 and 4F–4H). Therefore, we proposed that Ezh2 occupancy is weak at the IG-DMR, and it may be present in the vicinity of the locus in association with Gtl2 lncRNA. To address the mechanistic details of how Ezh2 prevents Dnmt3s occupancy/recruitment and DNAme at the IG-DMR locus, first we performed a time-course experiment after knockdown of Ezh2. Knockdown of Ezh2 showed reduced expression of Gtl2 lncRNA and increased expression of Dnmt3a (Figures S6A and S6B), similar to, but quantitatively less extreme than, the pattern observed upon complete deletion of Ezh2 (Figures 1D, 4B, S6A, and S6B). However, knockdown of Ezh2 did not increase the DNAme level at the IG-DMR, as we observed in *Ezh2*−/− mESCs (Figures S6C and 2C). On the other hand, deletion of *Dnmt3a* (*Dnmt3a*−/−) showed a modest increase in Gtl2 expression, but no significant change in DNAme at the IG-DMR (Figures S6D and S6E). In addition, depletion of Ezh2 in *Dnmt3a*−/− mESCs reduced Gtl2 expression (Figure S6F), indicating a positive function of Ezh2/PRC2 at the maternal *Gtl2-Rian-Mirg* locus.

Furthermore, we overexpressed Ezh2 and Dnmt3a in wild-type mESCs. Overexpression of neither Ezh2 nor Dnmt3a altered Gtl2 expression and DNAme at the IG-DMR (Figures 6A–6F). In addition, overexpression of Ezh2 in *Dnmt3a*−/− mESCs showed no significant change in Gtl2 expression and DNAme at the IG-DMR (Figures 6G–6I), implying that Ezh2 does not function as an activator at the IG-DMR locus. Taken together, these data support that Ezh2 functions to protect the IG-DMR locus from Dnmt3s/DNAme and, thereby, serves to maintain expression of the maternal *Gtl2-Rian-Mirg* locus.

DISCUSSION

The precise mechanisms regulating imprinting at the *Dlk1-Dio3* domain have remained largely unknown (da Rocha et al., 2008). Here we demonstrate that PRC2 is required for proper expression of the maternal *Gtl2-Rian-Mirg* locus, a cluster essential for successful iPSC reprogramming (Figure S7A; Stadtfeld et al., 2010). Absence of PRC2 results in markedly elevated DNAme at the IG-DMR, leading to transcriptional repression of the entire maternal *Gtl2-Rian-Mirg* locus (Figures 1 and 2). The maternal IG-DMR is lowly methylated/hypomethylated and acts as an enhancer of the maternal *Gtl2-Rian-Mirg* locus due to co-occupancy of ESC-specific TFs, mediators, cohesin, Lsd1, H3K27ac, and H3K4me1 (Figure 3). This finding is

Figure 3. IG-DMR/Enh1 Serves as an Enhancer for the *Gtl2-Rian-Mirg* Locus

(A–D) Co-occupancy of ESC-specific TFs (e.g., Oct4, Nanog, Sox2, Klf4, and Esrrb), mediator (Med1/12), cohesin (Smc1/3), Lsd1, H3K27ac, and H3K4me1 at IG-DMR/Enh1 and Enh2 fulfills criteria for putative enhancer regions of the *Gtl2-Rian-Mirg* locus (A). The magnified shaded regions show *Dlk1* promoter (B), IG-DMR/Enh1, *Gtl2* promoter (C), and Enh2 (D) regions, which are occupied with several factors and histones marks in *Ezh2*−/− and wild-type mESCs. Multiple individual ChIP-seq genomic tracks of PRC2 components show weak occupancy of Ezh2 and Jarid2 and no binding of Suz12 of PRC2 components at the IG-DMR/Enh1 and Enh2, and we failed to observe detectable H3K27me3 deposition.

(E) Luciferase reporter assays of Enh1 and Enh2 demonstrate strong enhancer activity as *Nanog* enhancer. Non-Enh1 and Non-Enh2 (lacks binding of any of the factors and histone marks, see Figure S3A) both were used as controls. Data are represented as mean ± SEM (n = 3); p values were calculated using a two-way ANOVA; ***p < 0.0001, **p < 0.001.

(F) Biallelic deletion of Enh2 (Enh2−/−) (~7 kb) reveals no effect on the *Gtl2-Rian-Mirg* locus, whereas, biallelic deletion of IG-DMR/Enh1 (IG-DMR/Enh1−/−) (~7 kb) abrogates expression of maternal Gtl2, Rian, and Mirg. Non-Enh2−/− (~7 kb) was used as a control. mRNA expression of Dlk1, Dio3, Gtl2, Rian, and Mirg were examined from undifferentiated wild-type, IG-DMR−/−, Enh2−/−, and Non-Enh2−/− mESCs. mRNA expressions are represented as mean ± SEM (n = 3); p values were calculated using a two-way ANOVA; ***p < 0.0001, **p < 0.001, *p < 0.01; ns, non-significant.

See also Figure S3.

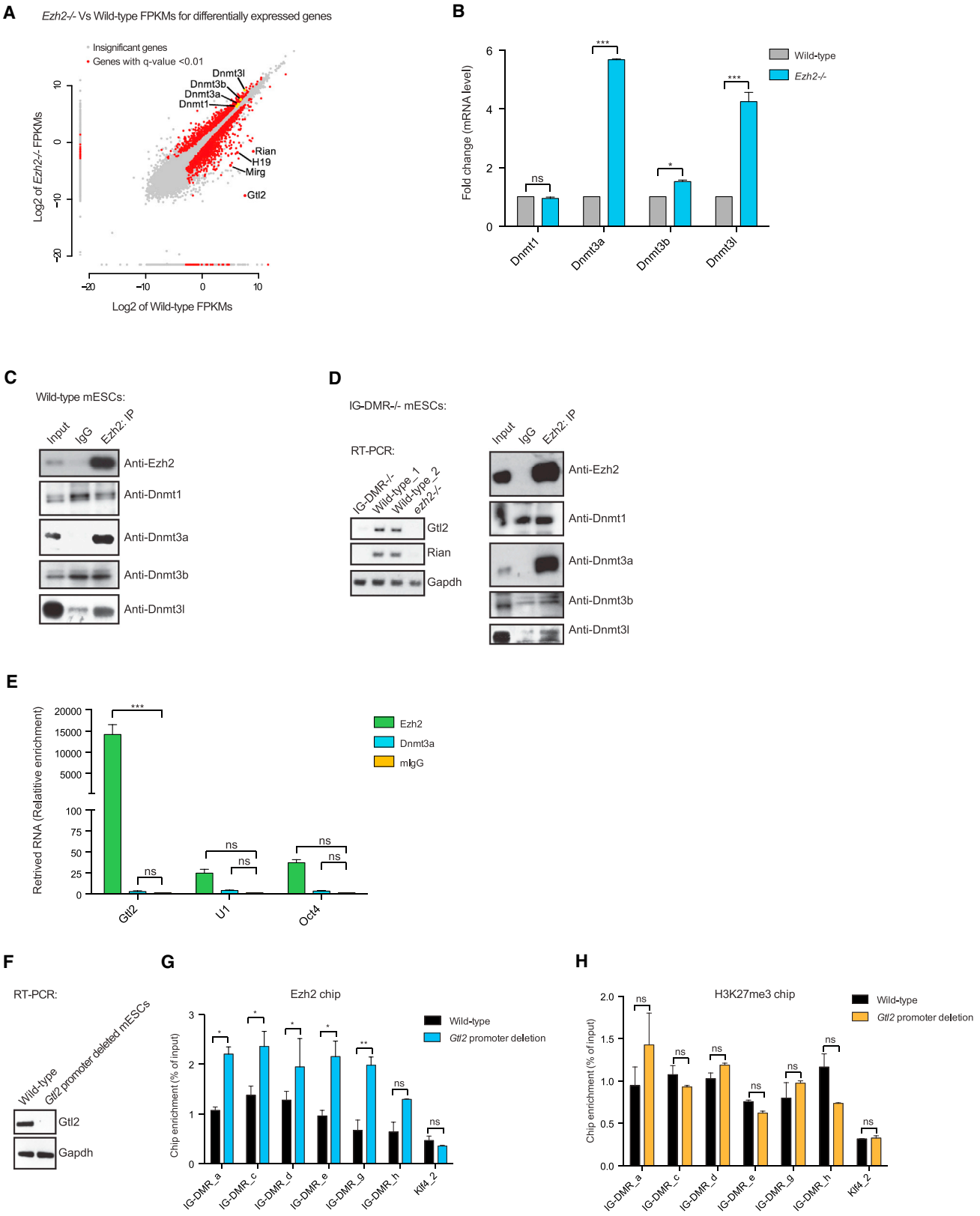

(legend on next page)

consistent with the observation that lowly methylated regions (LMRs) serve as distal regulatory regions and act as enhancers (Stadler et al., 2011).

Since Gtl2 lncRNA binds to Ezh2, the occupancy of Ezh2 is weak and H3K27me3 deposition does not take place at the IG-DMR of the maternal *Gtl2-Rian-Mirg* locus (Figures 3A, 3C, and 4E–4H). Nonetheless, we propose that the presence of Ezh2/PRC2 protects the IG-DMR locus from recruitment of Dnmt3s and subsequent DNAme. Several lines of evidence support this model. First, Ezh2 and Dnmt3a/3l physically interact (Figure 4C). Second, Dnmt3s binding to the IG-DMR is increased (Figures 5A and 5B) and DNA is strongly methylated in the absence of Ezh2 (and PRC2) (Figures 2C and 5C). Third, DNAme is globally increased at Ezh2-binding sites in the absence of Ezh2 (Figure 5D). Finally, neither overexpression of Ezh2 or Dnmt3a in wild-type ESCs nor overexpression of Ezh2 in *Dnmt3a*−/− ESCs alters DNAme at the IG-DMR and Gtl2 lncRNA expression (Figure 6). In effect, Ezh2/PRC2 then protects the IG-DMR locus from Dnmt3s and its activity (i.e., DNAme).

Generally the presence of Ezh2/PRC2 correlates with gene repression (Margueron and Reinberg, 2011). However, two recent reports demonstrated that PRC2 localizes not only at the promoter regions of repressed genes but also at the promoters of the active genes. Remarkably, PRC2 weakly occupies active promoter regions (with reduced level of H3K27me3) and binds to the 5′ terminus of nascent transcripts, which originate from active genes (Davidovich et al., 2013; Kaneko et al., 2013). These results suggest that PRC2 senses the transcription activity of genes through nascent RNA binding that tempers Ezh2/PRC2 activity (Kaneko et al., 2013). This scenario may allow continuous expression of active genes by cell-type-specific TFs, activators, despite the presence of PRC2. A similar phenomenon may drive continuous expression of the maternal *Gtl2-Rian-Mirg* locus in association with ESC-specific TFs, mediators, cohesion, H3K27ac, and H3K4me1 at the IG-DMR, despite the presence of Ezh2/PRC2 in association with Gtl2 lncRNA (Figure 7).

Our findings focus attention on the relationship of polycomb function and DNAme. Both pathways are involved in the establishment and maintenance of epigenetic gene silencing. Some evidence points to a cooperative relationship between DNAme and PRC2, where PRC2 facilitates binding (or recruitment) of Dnmts at PRC2 target promoters to promote DNAme (Viré et al., 2006). This scenario has been proposed in colon cancer, where Ezh2/PRC2 has been reported to recruit Dnmts for de novo DNAme to silence genes that are critical for normal colonic epithelium development (Schlesinger et al., 2007). Additionally, reduced levels of H3K27me3 and DNA hypomethylation concurrently activate gene expression in pediatric gliomas (Bender et al., 2013), implying that PRC2-mediated de novo DNAme contributes to carcinogenesis. In contrast, other evidence supports antagonism between DNAme and polycomb function. For example, genome-wide studies in mESCs revealed gain of H3K27me3 and DNAme upon loss of Dnmts and PRC2, respectively (Brinkman et al., 2012; Hagarman et al., 2013). Furthermore, developmentally related genes containing CpG islands that are silenced by PRC2 in normal cells acquire DNAme with loss of PRC2 marks in prostate cancer (Gal-Yam et al., 2008). Also, loss of Dnmt3a leads to an increased level of H3K27me3 in neural stem cells (Wu et al., 2010). Of particular note, a recent study implicated PRC2 in direct regulation of Dnmt3l (Basu et al., 2014), which is consistent with our observation of increased expression of Dnmt3s upon the loss of Ezh2/PRC2 (Figures 4A and 4B). In addition, links between DNA hypomethylation and accumulation and/or spreading of H3K27me3 have been proposed in cancer (Reddington et al., 2014). Thus, the relationship between DNAme and PRC2 may be critical in both normal and cancer cells.

Our data provide additional insights into the relationship between PRC2 and Dnmts. PRC2 interacts physically with Dnmt3a/3l in a Gtl2 lncRNA-independent manner and prevents Dnmt3s recruitment and subsequent DNAme at the IG-DMR of the maternal *Gtl2-Rian-Mirg* locus (Figures 4, 5, and 6). Dnmt3a/3l forms a tetramer for de novo DNAme (Jia et al., 2007). Dnmt3l shares homology with Dnmt3a and Dnmt3b, but lacks enzymatic activity, although Dnmt3l cooperates with Dnmt3a and Dnmt3b to establish maternal imprinting (Hata et al., 2002). Furthermore, Dnmt3l has been shown to enhance

Figure 4. PRC2 Physically Interacts with Dnmt3a/3l in a Gtl2 lncRNA-Independent Manner and the Interaction between Gtl2 lncRNA-Ezh2 Inhibits Binding of Ezh2/PRC2 at the IG-DMR

(A) Scatterplot representing differentially expressed genes from *Ezh2*−/− mESCs compared to wild-type. Red dots represent significantly up- and downregulated genes in *Ezh2*−/− mESCs with a q value < 0.01. Genes of interest are labeled in the scatterplot.

(B) The mRNA expression shows significant upregulation of Dnmt3a, Dnmt3b, and Dnmt3l, but not Dnmt1, in *Ezh2*−/− mESCs as compared to wild-type. Transcript levels were normalized to Gapdh. Data are represented as mean ± SEM (n = 3); p values were calculated using a two-way ANOVA; ***p < 0.0001, *p < 0.01; ns, non-significant.

(C) Anti-Ezh2 antibody was used to immunoprecipitate endogenous Ezh2 from mESC nuclear extracts, showing a specific interaction between Ezh2 and Dnmt3a/Dnmt3l.

(D) The qRT-PCR shows that biallelic deletion of IG-DMR−/− causes abrogation of maternal Gtl2 and Rian lncRNAs in mESCs. Endogenous Ezh2 maintains interaction with Dnmt3a/Dnmt3l in the absence of Gtl2 lncRNA.

(E) RNA immunoprecipitation (RIP) demonstrates a strong interaction of Gtl2 lncRNA with Ezh2, but not with Dnmt3a. U1 RNA and Oct4 mRNA were used as controls. Data are represented as mean ± SEM (n = 3); p values were calculated using a two-way ANOVA; ***p < 0.0001; ns, non-significant.

(F) The qRT-PCR shows that biallelic deletion of *Gtl2* promoter (~7 kb) disrupts the formation of Gtl2 lncRNA.

(G) ChIP-qPCR shows increased Ezh2 occupancy at the IG-DMR in the absence of Gtl2 lncRNA. Data are represented as mean ± SEM (n = 3); p values were calculated using a two-way ANOVA; **p < 0.001, *p < 0.01; ns, non-significant.

(H) ChIP-qPCR shows no significant increase in binding of H3K27me3 at the IG-DMR in the absence of Gtl2 lncRNA. Data are represented as mean ± SEM (n = 3); p values were calculated using a two-way ANOVA; ns, non-significant.

See also Figure S4.

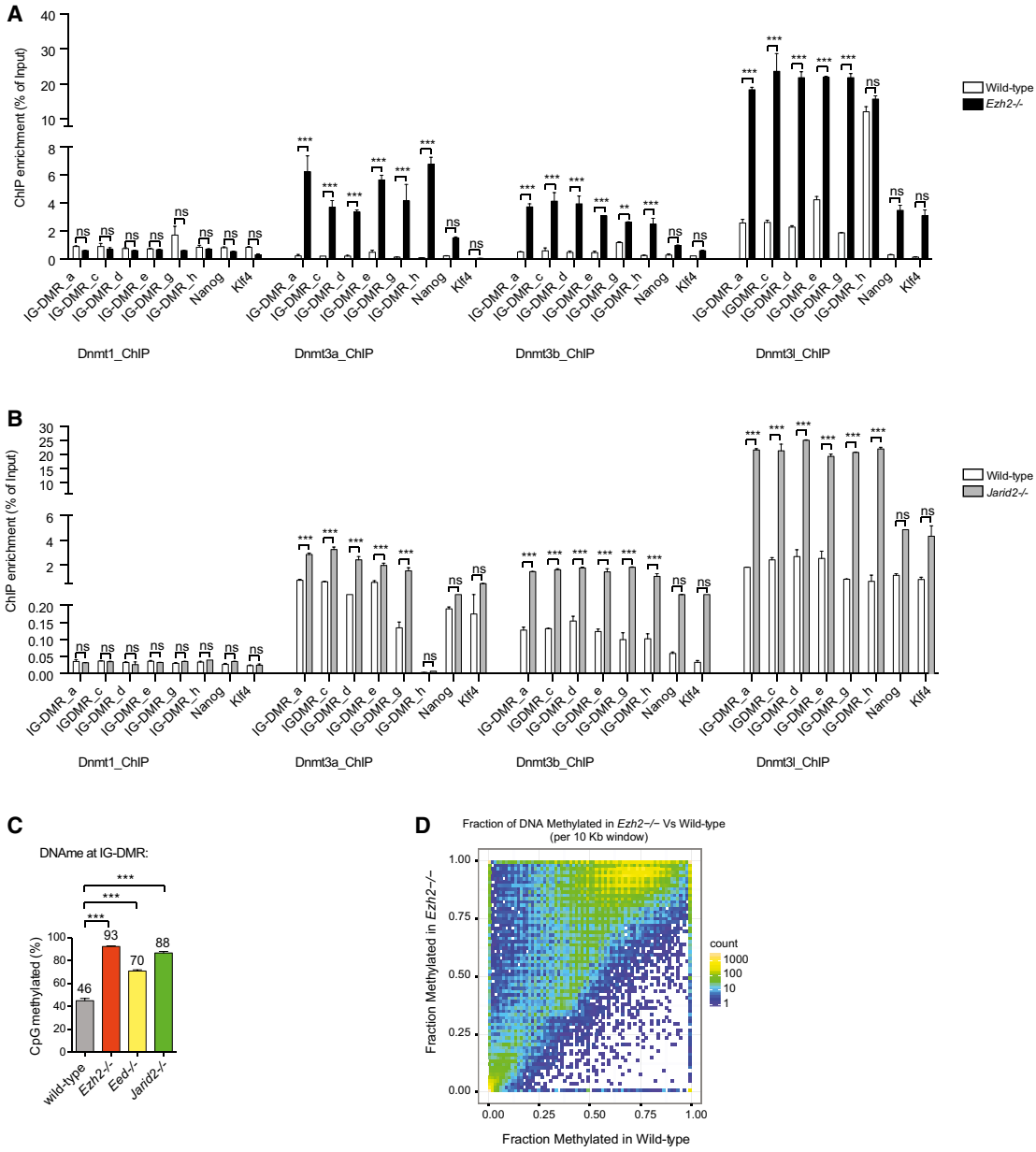

Figure 5. PRC2 Antagonizes De Novo DNAme at the IG-DMR through Distinct Mechanism

(A and B) ChIP-qPCR shows that Dnmt3a, Dnmt3b, and Dnmt3l occupancy at IG-DMR is significantly increased in the absence of Ezh2 (A) and Jarid2 (B), but occupancy of Dnmt1 remains unchanged. Data are represented as mean ± SEM (n = 3); p values were calculated using a two-way ANOVA; ***p < 0.0001; ns, non-significant.

(C) Analysis of 29 CpGs at the IG-DMR shows different DNAme (%) levels in the absence of PRC2 components. Data are represented as mean ± SEM (n = 3); p values were calculated using a two-way ANOVA; ***p < 0.0001.

(D) Global DNAme analysis from *Ezh2*−/− and wild-type mESCs, using reduced-representation bisulfite sequencing (RRBS), represented as a heatmap of genome-wide methylation patterns. The genome was divided into non-overlapping 10-kb windows and the fraction of methylated CpGs in each window was computed for wild-type and *Ezh2*−/− mutants. The hue represents the number of genomic windows with a given fractional methylation in *Ezh2*−/− versus wild-type. Trends suggest significantly increased global DNAme in *Ezh2*−/−.

See also Figure S5.

the de novo DNAme activity of Dnmt3a (Chedin et al., 2002), which implicates Dnmt3l as an important cofactor for Dnmt3a. In addition, conditional mutants of *Dnmt3a* and *Dnmt3l* in germs cells display indistinguishable phenotypes; however, conditional mutants of *Dnmt3b* demonstrate no apparent phenotype, indicating that Dnmt3a and Dnmt3l function together for DNAme at many of the imprinted loci in germ cells (Kaneda et al., 2004).

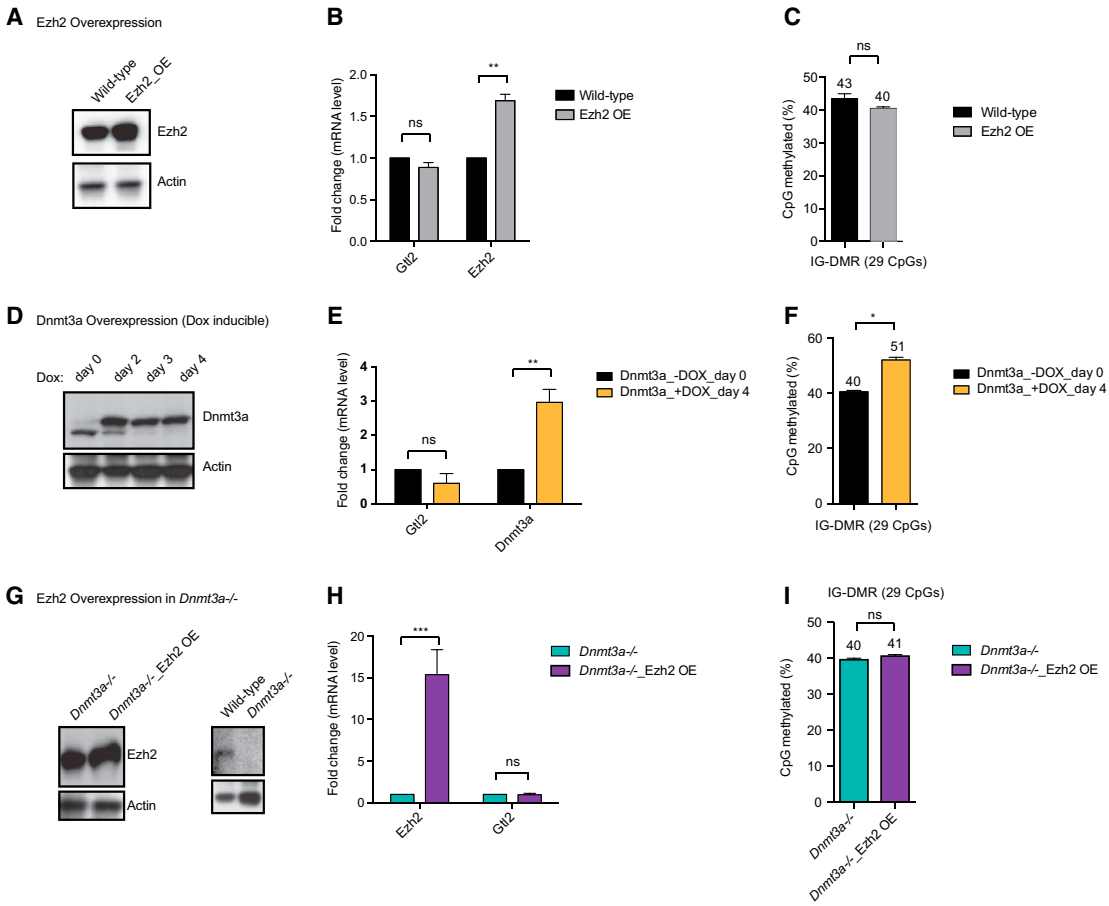

Figure 6. PRC2 Protects IG-DMR from De Novo DNAme to Allow Proper Expression of the Maternal *Gtl2-Rian-Mirg* Locus

(A) Overexpression of Ezh2 in wild-type mESCs. Protein expression of Ezh2 was checked through western blot. Actin was used as an internal control.

(B) The mRNA expression shows no significant change of Gtl2 lncRNA expression upon overexpression of Ezh2. Transcript levels were normalized to Gapdh. Data are represented as mean ± SEM (n = 3); p values were calculated using a two-way ANOVA; **p < 0.001; ns, non-significant.

(C) Analysis of 29 CpGs at the IG-DMR shows no significant changes of DNAme (%) levels upon overexpression of Ezh2. Data are represented as mean ± SEM (n = 3); p values were calculated using a two-way ANOVA; ns, non-significant.

(D–F) Dox-inducible overexpression of Dnmt3a (D, western blot) does not change Gtl2 lncRNA expression (qRT-PCR) (E), with a slight increase in DNAme level at the IG-DMR (F). Data are represented as mean ± SEM (n = 3); p values were calculated using a two-way ANOVA; **p < 0.001; ns, non-significant.

(G–I) Overexpression of Ezh2 in *Dnmt3a*−/− mESCs (G, western blot) leads to no significant change in Gtl2 lncRNA expression (qRT-PCR) (H) and DNAme at the IG-DMR (I). Data are represented as mean ± SEM (n = 3); p values were calculated using a two-way ANOVA; ***p < 0.0001; ns, non-significant.

See also Figure S6.

Although our findings are consistent with a model in which Ezh2 protects the IG-DMR locus from Dnmt3s recruitment and subsequent DNAme to maintain proper expression of the maternal *Gtl2-Rian-Mirg* locus, further study is needed to address more specific mechanistic issues. For one, it remains to be determined how and to what extent other PRC2 components, such as Eed, Suz12, and Jarid2, are involved in protecting the IG-DMR from DNAme. Second, the mechanism by which Gtl2 lncRNA inhibits binding of Ezh2/PRC2 at the IG-DMR and contributes to decreased H3K27me3 activity merits further clarification. Moreover, precisely how Gtl2 lncRNA recruits Ezh2/PRC2 at the IG-DMR and maintains its own expression through a feedback loop is not fully understood.

In conclusion, we find that Gtl2 lncRNA inhibits binding of Ezh2/PRC2 at the maternal IG-DMR locus, while Ezh2/PRC2 maintains its presence in the vicinity of the IG-DMR locus. In this manner, Ezh2/PRC2 protects the maternal IG-DMR locus by preventing recruitment of Dnmt3s and subsequent DNAme, thereby serving to maintain expression of the maternal *Gtl2-Rian-Mirg* locus in the presence of ESC-specific TFs and activators (Figure 7). In the absence of Ezh2, Dnmt3s is then recruited to and methylates the IG-DMR, leading to transcription repression of the maternal *Gtl2-Rian-Mirg* locus (Figure 7). Our findings also suggest that individual PRC2 components have different capacities to modulate Dnmt3s occupancy/recruitment and subsequent de novo DNAme at the IG-DMR (Figure 5), which ultimately sets different levels of expression of maternal lncRNAs and miRNAs from the *Gtl2-Rian-Mirg* locus (Figure 1). Collectively, our study provides a novel mechanism by which Ezh2/PRC2 antagonizes de novo DNAme at the IG-DMR for proper

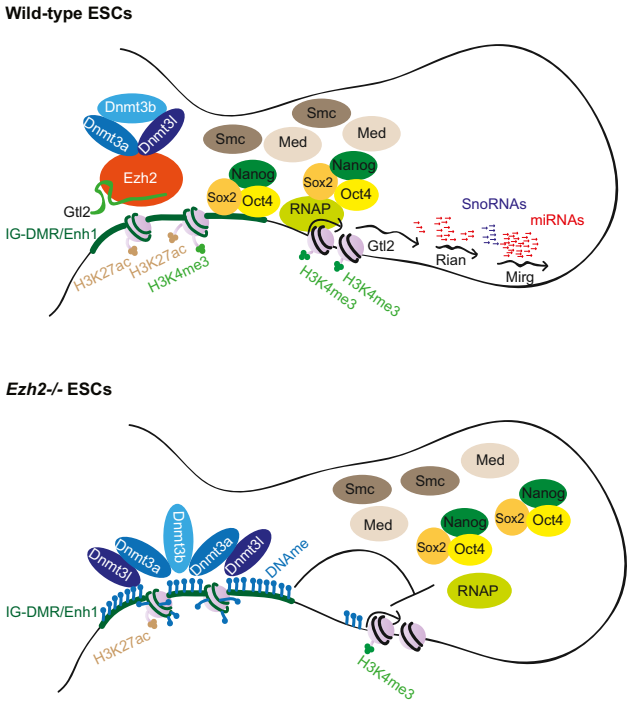

Figure 7. The Working Model Portrays the Mechanism by which Ezh2/PRC2 Protects the IG-DMR Locus from De Novo DNAme to Allow Proper Expression of the Maternal *Gtl2-Rian-Mirg* Locus in mESCs

A model schematically represents our findings, where Gtl2 lncRNA binds to Ezh2 and inhibits interaction of Ezh2/PRC2 at the IG-DMR locus and subsequent deposition of H3K27me3. The presence of Ezh2/PRC2 in association with Gtl2 lncRNA prevents Dnmt3s recruitment and subsequent de novo DNAme, and it allows ESC-specific TFs, mediators, and other histone modifiers to bind at the IG-DMR/Enh1 locus that ultimately drives expression of the maternal *Gtl2-Rian-Mirg* locus. In the absence Ezh2, it is unable to prevent recruitment of Dnmt3s at the IG-DMR locus. Dnmt3s is then recruited to the IG-DMR and deposits de novo DNAme, leading to transcription repression of the maternal *Gtl2-Rian-Mirg* locus. Significant reduction of H3K27ac and H3K4me3 occupancy at the IG-DMR and *Gtl2* promoter is observed in the absence of Ezh2. For simplicity, only the maternal allele is shown.

expression of the maternal *Gtl2-Rian-Mirg* locus, a critical region essential for mESC identity and somatic cell reprogramming (Pereira et al., 2010; Stadtfeld et al., 2010).

EXPERIMENTAL PROCEDURES

mESC Culture

Mouse CJ7 (wild-type), *Ezh2*−/−, *Eed*−/−, *Jarid2*−/−, and other mESC lines were maintained in the following ES medium: DMEM (Life Technologies) supplemented with 15% fetal calf serum (Life Technologies), 0.1 mM β-mercaptoethanol (Sigma), 2 mM L-glutamine (Life Technologies), 0.1 mM nonessential amino acid (Life Technologies), 1% nucleoside mix (Sigma), 1,000 U/ ml recombinant leukemia inhibitory factor (LIF, Chemicon), and 50 U/ml penicillin/streptomycin (Life Technologies). *Ezh2*−/−, *Eed*−/−, and *Jarid2*−/− mESCs were established previously (Shen et al., 2008, 2009; Xie et al., 2014).

Small RNA-Seq

Total RNA was isolated from undifferentiated mESCs using Trizol reagent (Invitrogen) according to the manufacturer's instructions. Total RNA (10 μg) from CJ7 (wild-type), *Ezh2*−/−, *Eed*−/−, and *Jarid2*−/− mESCs were size selected to 18–40 nt on a denaturing polyacrylamide gel, and small RNA libraries were prepared according to the manufacturer's instructions (SOLiD small RNA library preparation kit, Life Technologies). All libraries were sequenced using SOLiD instrument (Life Technologies).

RNA-Seq

Total RNA was isolated from undifferentiated mESCs using Trizol reagent (Invitrogen) according to the manufacturer's instructions. Total RNA (1 μg) was used from CJ7 (wild-type), *Ezh2*−/−, *Eed*−/−, and *Jarid2*−/− mESCs to prepare the mRNA libraries according to the manufacturer's instructions (Directional [strand-specific] mRNA-Seq sample preparation kit, Illumina). All libraries were sequenced using HiSeq 2000 sequencing system (Illumina).

Northern Blot

Total RNA (10 μg) was resolved in denaturing PAGE, transferred to a nitrocellulose membrane, and hybridized with DNA or locked nucleic acid (LNA) probes specific to each miRNA, as described previously (Das et al., 2008).

qRT-PCR

Total RNA was isolated from mESCs using RNeasy plus kit (QIAGEN) or Trizol (Invitrogen) and treated with DNaseI (Life Technologies) to remove the DNA contamination. RNA was converted to cDNA with a cDNA synthesis kit (Bio-Rad). The qRT-PCR was performed with SYBR green master mix (Bio-Rad) on Bio-Rad iCycler RT-PCR detection system according to the manufacturer's instructions. Small RNA RT-PCR was performed using Taqman miRNA assays (Life Technologies) as described previously (Das et al., 2008).

ChIP

ChIP was performed as described elsewhere (Das et al., 2014). Detailed procedures and a list of antibodies are available in the Supplemental Experimental Procedures.

ChIP-Seq and Library Generation

Purified ChIP DNA was used to prepare Illumina multiplexed sequencing libraries. New England Biolabs next-generation sequencing kit was used to prepare the libraries.

ChIP-Seq Data Analyses

All ChIP-seq samples were aligned with Bowtie v0.12.9 to the mm9 genome assembly, where only uniquely mappable reads were reported. Significant peaks were found by pairing each ChIP-seq sample with the appropriate input and running SICER v1.1, with a false discovery rate (FDR) of 0.05. See the Supplemental Experimental Procedures for more detail.

DNAme Analysis

Genomic DNA was bisulphate converted and analyzed by EpigenDx using the following assays: IG-DMR (ADS-1452), Oct4 promoter (ASY-585), and Nanog promoter (ASY-590).

ACCESSION NUMBERS

The accession number for the RNA-seq, small RNA-seq, ChIP-seq, and microarray data reported in this paper is GEO: GSE58414.

SUPPLEMENTAL INFORMATION

Supplemental Information includes Supplemental Experimental Procedures, seven figures, and seven tables and can be found with this article online at http://dx.doi.org/10.1016/j.celrep.2015.07.053.

AUTHOR CONTRIBUTIONS

P.P.D. and S.H.O. designed the experiments. P.P.D., E.A., A.H.B., S.B., D.L., H.X., D.L.J.J., M.C.C., J.C., J.X., Y.Z., W.K., A.D.L.A., and X.S. performed the

experiments. P.P.D., D.A.H., R. Karnik, R. Kuintzle, and Z.S. analyzed the data. P.P.D., D.A.H., A.M., K.H., M.K., G.Q.D., R.I.G., J.K., and S.H.O interpreted the data. P.P.D., D.A.H., and S.H.O. wrote the manuscript.

ACKNOWLEDGMENTS

We thank Pratibha Tripathi; Glenn MacLean for reagents; Fieda Abderazzaq and Renee Rubio at the Center for Cancer Computational Biology (CCCB) sequencing facility, DFCI, for Illumina HiSeq2000 Sequencing; and the late Edward Fox at the Microarray Core of DFCI for microarray and small RNA-seq. This work was supported by funding from NIH grant HLBI U01HL100001. S.H.O. is an Investigator of the HHMI. M.C.C. was supported by NIH grant F30 DK103359-01A1.

Received: March 13, 2015
Revised: July 19, 2015
Accepted: July 27, 2015
Published: August 20, 2015

REFERENCES

Basu, A., Dasari, V., Mishra, R.K., and Khosla, S. (2014). The CpG island encompassing the promoter and first exon of human DNMT3L gene is a PcG/TrX response element (PRE). PLoS ONE *9*, e93561.

Bender, S., Tang, Y., Lindroth, A.M., Hovestadt, V., Jones, D.T.W., Kool, M., Zapatka, M., Northcott, P.A., Sturm, D., Wang, W., et al. (2013). Reduced H3K27me3 and DNA hypomethylation are major drivers of gene expression in K27M mutant pediatric high-grade gliomas. Cancer Cell *24*, 660–672.

Bernstein, B.E., Mikkelsen, T.S., Xie, X., Kamal, M., Huebert, D.J., Cuff, J., Fry, B., Meissner, A., Wernig, M., Plath, K., et al. (2006). A bivalent chromatin structure marks key developmental genes in embryonic stem cells. Cell *125*, 315–326.

Boyer, L.A., Plath, K., Zeitlinger, J., Brambrink, T., Medeiros, L.A., Lee, T.I., Levine, S.S., Wernig, M., Tajonar, A., Ray, M.K., et al. (2006). Polycomb complexes repress developmental regulators in murine embryonic stem cells. Nature *441*, 349–353.

Brinkman, A.B., Gu, H., Bartels, S.J.J., Zhang, Y., Matarese, F., Simmer, F., Marks, H., Bock, C., Gnirke, A., Meissner, A., and Stunnenberg, H.G. (2012). Sequential ChIP-bisulfite sequencing enables direct genome-scale investigation of chromatin and DNA methylation cross-talk. Genome Res. *22*, 1128–1138.

Brookes, E., de Santiago, I., Hebenstreit, D., Morris, K.J., Carroll, T., Xie, S.Q., Stock, J.K., Heidemann, M., Eick, D., Nozaki, N., et al. (2012). Polycomb associates genome-wide with a specific RNA polymerase II variant, and regulates metabolic genes in ESCs. Cell Stem Cell *10*, 157–170.

Chedin, F., Lieber, M.R., and Hsieh, C.-L. (2002). The DNA methyltransferase-like protein DNMT3L stimulates de novo methylation by Dnmt3a. Proc. Natl. Acad. Sci. USA *99*, 16916–16921.

Cong, L., Ran, F.A., Cox, D., Lin, S., Barretto, R., Habib, N., Hsu, P.D., Wu, X., Jiang, W., Marraffini, L.A., and Zhang, F. (2013). Multiplex genome engineering using CRISPR/Cas systems. Science *339*, 819–823.

da Rocha, S.T., Edwards, C.A., Ito, M., Ogata, T., and Ferguson-Smith, A.C. (2008). Genomic imprinting at the mammalian Dlk1-Dio3 domain. Trends Genet. *24*, 306–316.

Das, P.P., Bagijn, M.P., Goldstein, L.D., Woolford, J.R., Lehrbach, N.J., Sapetschnig, A., Buhecha, H.R., Gilchrist, M.J., Howe, K.L., Stark, R., et al. (2008). Piwi and piRNAs act upstream of an endogenous siRNA pathway to suppress Tc3 transposon mobility in the Caenorhabditis elegans germline. Mol. Cell *31*, 79–90.

Das, P.P., Shao, Z., Beyaz, S., Apostolou, E., Pinello, L., De Los Angeles, A., O'Brien, K., Atsma, J.M., Fujiwara, Y., Nguyen, M., et al. (2014). Distinct and combinatorial functions of Jmjd2b/Kdm4b and Jmjd2c/Kdm4c in mouse embryonic stem cell identity. Mol. Cell *53*, 32–48.

Davidovich, C., Zheng, L., Goodrich, K.J., and Cech, T.R. (2013). Promiscuous RNA binding by Polycomb repressive complex 2. Nat. Struct. Mol. Biol. *20*, 1250–1257.

Dong, K.B., Maksakova, I.A., Mohn, F., Leung, D., Appanah, R., Lee, S., Yang, H.W., Lam, L.L., Mager, D.L., Schübeler, D., et al. (2008). DNA methylation in ES cells requires the lysine methyltransferase G9a but not its catalytic activity. EMBO J. *27*, 2691–2701.

Edwards, C.A., and Ferguson-Smith, A.C. (2007). Mechanisms regulating imprinted genes in clusters. Curr. Opin. Cell Biol. *19*, 281–289.

Epsztejn-Litman, S., Feldman, N., Abu-Remaileh, M., Shufaro, Y., Gerson, A., Ueda, J., Deplus, R., Fuks, F., Shinkai, Y., Cedar, H., and Bergman, Y. (2008). De novo DNA methylation promoted by G9a prevents reprogramming of embryonically silenced genes. Nat. Struct. Mol. Biol. *15*, 1176–1183.

Ferrari, K.J., Scelfo, A., Jammula, S., Cuomo, A., Barozzi, I., Stützer, A., Fischle, W., Bonaldi, T., and Pasini, D. (2014). Polycomb-dependent H3K27me1 and H3K27me2 regulate active transcription and enhancer fidelity. Mol. Cell *53*, 49–62.

Gal-Yam, E.N., Egger, G., Iniguez, L., Holster, H., Einarsson, S., Zhang, X., Lin, J.C., Liang, G., Jones, P.A., and Tanay, A. (2008). Frequent switching of Polycomb repressive marks and DNA hypermethylation in the PC3 prostate cancer cell line. Proc. Natl. Acad. Sci. USA *105*, 12979–12984.

Hagarman, J.A., Motley, M.P., Kristjansdottir, K., and Soloway, P.D. (2013). Coordinate regulation of DNA methylation and H3K27me3 in mouse embryonic stem cells. PLoS ONE *8*, e53880.

Hata, K., Okano, M., Lei, H., and Li, E. (2002). Dnmt3L cooperates with the Dnmt3 family of de novo DNA methyltransferases to establish maternal imprints in mice. Development *129*, 1983–1993.

Jia, D., Jurkowska, R.Z., Zhang, X., Jeltsch, A., and Cheng, X. (2007). Structure of Dnmt3a bound to Dnmt3L suggests a model for de novo DNA methylation. Nature *449*, 248–251.

Kagey, M.H., Newman, J.J., Bilodeau, S., Zhan, Y., Orlando, D.A., van Berkum, N.L., Ebmeier, C.C., Goossens, J., Rahl, P.B., Levine, S.S., et al. (2010). Mediator and cohesin connect gene expression and chromatin architecture. Nature *467*, 430–435.

Kaneda, M., Okano, M., Hata, K., Sado, T., Tsujimoto, N., Li, E., and Sasaki, H. (2004). Essential role for de novo DNA methyltransferase Dnmt3a in paternal and maternal imprinting. Nature *429*, 900–903.

Kaneko, S., Son, J., Shen, S.S., Reinberg, D., and Bonasio, R. (2013). PRC2 binds active promoters and contacts nascent RNAs in embryonic stem cells. Nat. Struct. Mol. Biol. *20*, 1258–1264.

Kaneko, S., Son, J., Bonasio, R., Shen, S.S., and Reinberg, D. (2014). Nascent RNA interaction keeps PRC2 activity poised and in check. Genes Dev. *28*, 1983–1988.

Kanhere, A., Viiri, K., Araújo, C.C., Rasaiyaah, J., Bouwman, R.D., Whyte, W.A., Pereira, C.F., Brookes, E., Walker, K., Bell, G.W., et al. (2010). Short RNAs are transcribed from repressed polycomb target genes and interact with polycomb repressive complex-2. Mol. Cell *38*, 675–688.

Ku, M., Koche, R.P., Rheinbay, E., Mendenhall, E.M., Endoh, M., Mikkelsen, T.S., Presser, A., Nusbaum, C., Xie, X., Chi, A.S., et al. (2008). Genomewide analysis of PRC1 and PRC2 occupancy identifies two classes of bivalent domains. PLoS Genet. *4*, e1000242.

Lin, S.-P., Youngson, N., Takada, S., Seitz, H., Reik, W., Paulsen, M., Cavaille, J., and Ferguson-Smith, A.C. (2003). Asymmetric regulation of imprinting on the maternal and paternal chromosomes at the Dlk1-Gtl2 imprinted cluster on mouse chromosome 12. Nat. Genet. *35*, 97–102.

Margueron, R., and Reinberg, D. (2011). The Polycomb complex PRC2 and its mark in life. Nature *469*, 343–349.

Mikkelsen, T.S., Ku, M., Jaffe, D.B., Issac, B., Lieberman, E., Giannoukos, G., Alvarez, P., Brockman, W., Kim, T.-K., Koche, R.P., et al. (2007). Genome-wide maps of chromatin state in pluripotent and lineage-committed cells. Nature *448*, 553–560.

Pandey, R.R., Mondal, T., Mohammad, F., Enroth, S., Redrup, L., Komorowski, J., Nagano, T., Mancini-Dinardo, D., and Kanduri, C. (2008). Kcnq1ot1

antisense noncoding RNA mediates lineage-specific transcriptional silencing through chromatin-level regulation. Mol. Cell *32*, 232–246.

Pereira, C.F., Piccolo, F.M., Tsubouchi, T., Sauer, S., Ryan, N.K., Bruno, L., Landeira, D., Santos, J., Banito, A., Gil, J., et al. (2010). ESCs require PRC2 to direct the successful reprogramming of differentiated cells toward pluripotency. Cell Stem Cell *6*, 547–556.

Reddington, J.P., Sproul, D., and Meehan, R.R. (2014). DNA methylation reprogramming in cancer: does it act by re-configuring the binding landscape of Polycomb repressive complexes? BioEssays *36*, 134–140.

Rinn, J.L., Kertesz, M., Wang, J.K., Squazzo, S.L., Xu, X., Brugmann, S.A., Goodnough, L.H., Helms, J.A., Farnham, P.J., Segal, E., and Chang, H.Y. (2007). Functional demarcation of active and silent chromatin domains in human HOX loci by noncoding RNAs. Cell *129*, 1311–1323.

Schlesinger, Y., Straussman, R., Keshet, I., Farkash, S., Hecht, M., Zimmerman, J., Eden, E., Yakhini, Z., Ben-Shushan, E., Reubinoff, B.E., et al. (2007). Polycomb-mediated methylation on Lys27 of histone H3 pre-marks genes for de novo methylation in cancer. Nat. Genet. *39*, 232–236.

Shen, X., Liu, Y., Hsu, Y.-J., Fujiwara, Y., Kim, J., Mao, X., Yuan, G.-C., and Orkin, S.H. (2008). EZH1 mediates methylation on histone H3 lysine 27 and complements EZH2 in maintaining stem cell identity and executing pluripotency. Mol. Cell *32*, 491–502.

Shen, X., Kim, W., Fujiwara, Y., Simon, M.D., Liu, Y., Mysliwiec, M.R., Yuan, G.-C., Lee, Y., and Orkin, S.H. (2009). Jumonji modulates polycomb activity and self-renewal versus differentiation of stem cells. Cell *139*, 1303–1314.

Simon, J.A., and Kingston, R.E. (2009). Mechanisms of polycomb gene silencing: knowns and unknowns. Nat. Rev. Mol. Cell Biol. *10*, 697–708.

Smith, Z.D., and Meissner, A. (2013). DNA methylation: roles in mammalian development. Nat. Rev. Genet. *14*, 204–220.

Stadler, M.B., Murr, R., Burger, L., Ivanek, R., Lienert, F., Schöler, A., van Nimwegen, E., Wirbelauer, C., Oakeley, E.J., Gaidatzis, D., et al. (2011). DNA-binding factors shape the mouse methylome at distal regulatory regions. Nature *480*, 490–495.

Stadtfeld, M., Apostolou, E., Akutsu, H., Fukuda, A., Follett, P., Natesan, S., Kono, T., Shioda, T., and Hochedlinger, K. (2010). Aberrant silencing of imprinted genes on chromosome 12qF1 in mouse induced pluripotent stem cells. Nature *465*, 175–181.

Stadtfeld, M., Apostolou, E., Ferrari, F., Choi, J., Walsh, R.M., Chen, T., Ooi, S.S.K., Kim, S.Y., Bestor, T.H., Shioda, T., et al. (2012). Ascorbic acid prevents loss of Dlk1-Dio3 imprinting and facilitates generation of all-iPS cell mice from terminally differentiated B cells. Nat. Genet. *44*, 398–405, S1–S2.

Takahashi, K., and Yamanaka, S. (2006). Induction of pluripotent stem cells from mouse embryonic and adult fibroblast cultures by defined factors. Cell *126*, 663–676.

Viré, E., Brenner, C., Deplus, R., Blanchon, L., Fraga, M., Didelot, C., Morey, L., Van Eynde, A., Bernard, D., Vanderwinden, J.-M., et al. (2006). The Polycomb group protein EZH2 directly controls DNA methylation. Nature *439*, 871–874.

Whyte, W.A., Bilodeau, S., Orlando, D.A., Hoke, H.A., Frampton, G.M., Foster, C.T., Cowley, S.M., and Young, R.A. (2012). Enhancer decommissioning by LSD1 during embryonic stem cell differentiation. Nature *482*, 221–225.

Wu, H., Coskun, V., Tao, J., Xie, W., Ge, W., Yoshikawa, K., Li, E., Zhang, Y., and Sun, Y.E. (2010). Dnmt3a-dependent nonpromoter DNA methylation facilitates transcription of neurogenic genes. Science *329*, 444–448.

Xie, W., Barr, C.L., Kim, A., Yue, F., Lee, A.Y., Eubanks, J., Dempster, E.L., and Ren, B. (2012). Base-resolution analyses of sequence and parent-of-origin dependent DNA methylation in the mouse genome. Cell *148*, 816–831.

Xie, H., Xu, J., Hsu, J.H., Nguyen, M., Fujiwara, Y., Peng, C., and Orkin, S.H. (2014). Polycomb repressive complex 2 regulates normal hematopoietic stem cell function in a developmental-stage-specific manner. Cell Stem Cell *14*, 68–80.

Zhao, J., Sun, B.K., Erwin, J.A., Song, J.J., and Lee, J.T. (2008). Polycomb proteins targeted by a short repeat RNA to the mouse X chromosome. Science *322*, 750–756.

Zhao, J., Ohsumi, T.K., Kung, J.T., Ogawa, Y., Grau, D.J., Sarma, K., Song, J.J., Kingston, R.E., Borowsky, M., and Lee, J.T. (2010). Genome-wide identification of polycomb-associated RNAs by RIP-seq. Mol. Cell *40*, 939–953.

Zhou, V.W., Goren, A., and Bernstein, B.E. (2011). Charting histone modifications and the functional organization of mammalian genomes. Nat. Rev. Genet. *12*, 7–18.